IR Spectra and Vibrational Modes of the Hydrofluoroethers CF_3OCH_3, CF_3OCF_2H, and $CF_3OCF_2CF_2H$ and Corresponding Alkanes CF_3CH_3, CF_3CF_2H, and $CF_3CF_2CF_2H$

Jonathan E. Stevens*, Lindsey D. Macomber and Lauren W. Davis

University of Detroit Mercy, Detroit MI 48219-3038, USA

Abstract: The structures and IR spectra of CF_3OCH_3, CF_3OCF_2H, and $CF_3OCF_2CF_2H$ and corresponding alkanes CF_3CH_3, CF_3CF_2H, and $CF_3CF_2CF_2H$ have been calculated using the B3LYP method with a 6-311G(2d,2p) basis set. The calculated IR spectra are consistent with, and provide additional confidence in, the available experimental data.

INTRODUCTION

The use of chlorofluorocarbons (CFCs) and Halons as refrigerant or heat transfer fluids leads to their emission into the atmosphere where they contribute to stratospheric ozone depletion [1, 2]. Over the past 10-20 years there has been an international effort to replace these compounds with environmentally acceptable alternatives. Hydrofluoroethers (HFEs) are one class of replacement compounds. These compounds do not contain chlorine or bromine and do not contribute to stratospheric ozone destruction [3]. Young *et al.* [3] have noted that the "atmospheric window" or range of infrared (IR) wavelengths that can easily escape the atmosphere is between 750 and 1250 cm^{-1} and that typical C-O and C-F vibrational stretching modes absorb in this range. The atmospheric lifetime of fluorinated ethers can be relatively long [3] with lifetimes increasing with the degree of fluorination [4,5] allowing longer times for these compounds to absorb radiation and contribute to radiative forcing of climate change.

The Global Warming Potential (GWP) of a fluorinated ether thus depends on its radiative forcing value, which is a function of its infrared spectrum, and upon its atmospheric lifetime [6-8]. Computational studies have predicted the IR spectra of several fluorinated ethers and provided estimates of radiative forcings [7-10]. Information on lifetimes has come from several recent kinetics experiments [4,11-13]. Lifetime estimates may also be based on computational studies of thermodynamic properties [7,14].

The relationship between the molecular structure of fluorinated ethers and their ability to absorb radiation has been a subject of recent study. Recent work by Young *et al.* [5] has developed a quantitative relationship between molecular structure and radiative efficiency. Good and Francisco [7] studied the theoretical IR spectra of the compounds CHF_2OCF_3 (E125), CHF_2OCHF_2 (E134), and CH_3OCF_3 (E143A) as determined by intensive *ab initio*

electronic structure calculations; their observations indicated that absorption of IR within the "atmospheric window" would occur for the compounds they studied, and that further, increases in the degree of fluorine substitution increased the quantity of absorption within the window wavelengths.

The work of Francisco does not specifically address the impact of the inclusion of the O atom upon absorptions in the window- i.e., it does not consider spectrum of the ether in comparison to that of the analogous alkane (where "analogous" means the alkane that would be obtained by removing an oxygen atom from the ether formula). Fluorinated alkanes, or hydrofluorocarbons (HFCs), are believed to have even longer lifetimes than HFEs [9,11-14]. Though some concerns exist about their presence as pollutants in the troposphere [15], HFCs are currently used as CFC replacements [7,15]. It has been postulated that HFEs have a lower global warming potential than the HFCs they would replace [7]. Assessment of the relative global warming potential of HFCs and HFEs requires knowledge of atmospheric lifetimes and the infrared absorption characteristics of both.

In this work, we present for comparison the computed structures and IR spectra of several fluorinated ethers and their analogous alkanes in the gas phase. IR spectra are compared to experimental data; T.J. Wallington of Ford Motor Company has provided experimental IR absorption spectra of fluorinated ethers and analogous alkanes to our group. The collection of the experimental data is described and spectra for these compounds are presented in several recent publications [16-18].

The following section describes our computations. Then our results section displays and compare the experimental and theoretical spectra. The results section also includes our predictions on the structure and relative energies of the conformers of these compounds, and data on the nuclear motions associated with each vibrational mode. In the conclusions section, this latter information is discussed with respect to the computed intensity of the modes.

*Address correspondence to this author at the University of Detroit Mercy, Detroit MI 48219-3038, USA; Tel: 313-993-1048; Fax: 313-993-1144; E-mail: stevenje@udmercy.edu

COMPUTATIONAL METHODS

The structures of ethers CF_3OCH_3, CF_3OCF_2H, and $CF_3OCF_2CF_2H$ and of the corresponding alkanes CF_3CH_3, CF_3CF_2H, and $CF_3CF_2CF_2H$ were optimized with the B3LYP [19] method and a 6-311G(2d,2p) basis set. All optimizations were initiated assuming asymmetric structures and then re-optimized in the appropriate point group (if other than C_1). Frequency calculations verified that all optimized structures were minima and vibrational zero point energies are incorporated into all relative energies reported here. The *Gaussian 03* electronic structure software package [20] was used for all calculations.

RESULTS

Fig. (**1**) displays the optimized structures of CF_3OCH_3 and CF_3OCF_2H as well as structures of the analogous alkanes. The structure of CF_3OCH_3 is very similar to those optimized by the intensive computations of Good and Francisco [7]; our results concur with theirs that the molecule has one conformer belonging to the C_s point group. The analogous alkane, CF_3CH_3, belongs to the C_{3v} point group.

Optimizations found CF_3OCF_2H to exist in two stable conformers, as displayed in Fig. (**1**) Conformer #2 is the more stable, with a relative energy of -1.02 kcal/mol compared to conformer #1. Neither structure has elements of symmetry and consequently both belong to the C_1 point group. Both conformers are distorted from C_s symmetry by

rotations of the terminal methyl groups. Conformer 1, for example, exhibits a FCOC dihedral of 165.0 degrees for a -CF_3 fluorine which would be expected to have a FCOC dihedral of 180 in C_s symmetry. Likewise, the hydrogen attached to the -CF_2H group has an HCOC dihedral angle of 167.0 degrees instead of the idealized value of 180 required for C_s symmetry. The calculations find one conformer of CF_3CF_2H, belonging to the C_s point group.

Optimized structures of $CF_3OCF_2CF_2H$ and its analogous alkane appear in Fig. (**2**). Computations find two conformers of $CF_3OCF_2CF_2H$; conformer 1 is characterized by deformation of the ideally planar carbon-oxygen backbone (with COCC dihedral angle of -164.6), rotation of the -CF_3 group directly attached to the O, and a -CF_2H terminal hydrogen in the *gauche* position. On the terminal -CF_3, a FCOC dihedral is approximately 160 degrees, as opposed to the idealized value of 180 degrees. Conformer #2 has a relative energy of - 0.016 kcal/mol relative to conformer #1. The primary difference between this conformer and conformer #1 is placement of the hydrogen in the terminal -CF_2H group in an *anti* position as opposed to a *gauche* one. There is a similar distortion of the C-OCC backbone (dihedral angle 164.0) and the -CF_3 group exhibits a rotation similar to the rotation found in conformer #1,with a FCOC dihedral angle of approximately 160 degrees.

Calculations likewise find two conformers for $CF_3CF_2CF_2H$. Conformer #1, with anti placement of the hydrogen, is the more stable. Conformer #2 exhibits *gauche*
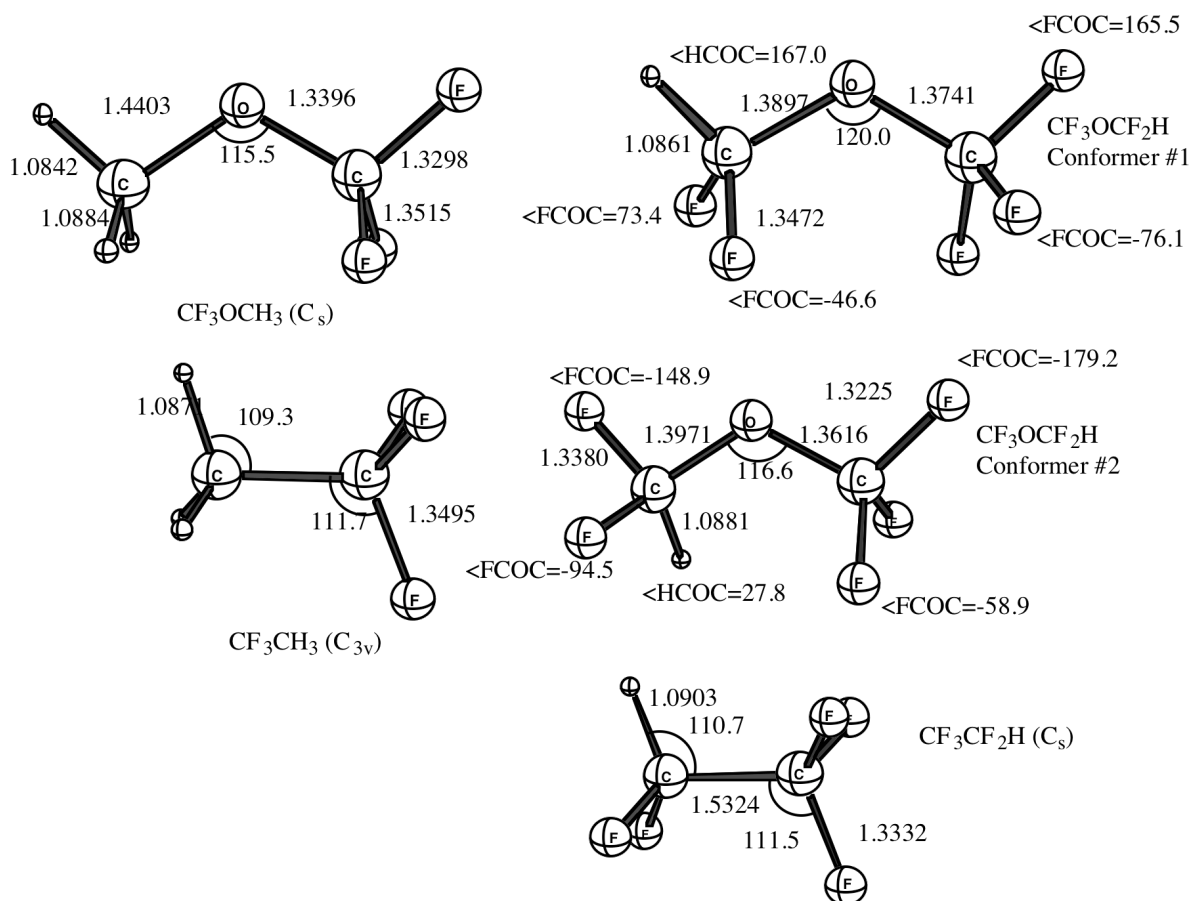

Fig. (1). Structures of CF_3OCH_3,CF_3CH_3, CF_3OCF_2H, and CF_3CF_2H optimized with B3LYP/6-311G(2d,2p) calculations. All bond lengths are in angstroms (Å) and all angles are in degrees.

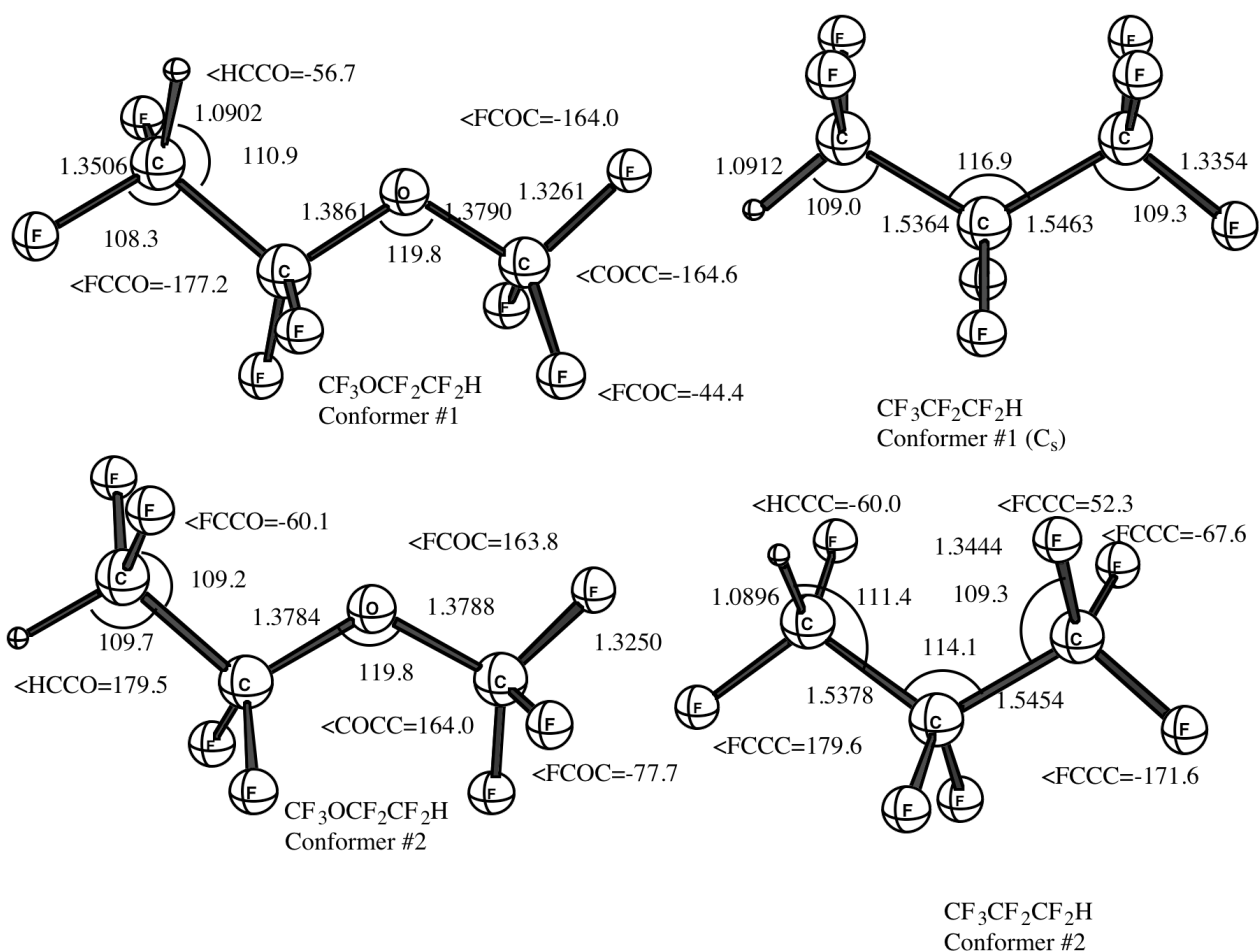**Fig. (2).** Structures of $CF_3OCF_2CF_2H$ and $CF_3CF_2CF_2H$ optimized with B3LYP/6-311G(2d,2p) calculations. All bond lengths are in angstroms (Å) and all angles are in degrees.

placement of the hydrogen and has an energy of 0.020 kcal/mol relative to conformer #1. There is a slight rotation of the terminal -CF_3 group as indicated by the dihedral angles presented in Fig. (**2**).

Tables **1-6** display the vibrational data for CF_3OCH_3, CF_3CH_3, CF_3OCF_2H, CF_3CF_2H, $CF_3OCF_2CF_2H$, and $CF_3CF_2CF_2H$. Examination of the data reveals that each ether has 3 more vibrational modes than the corresponding alkane, as you would expect given the 3N-6 rule for the number of vibrational modes of a nonlinear molecule. The brightest or most intense modes in the ether are more intense that the brightest modes of the corresponding alkane; the computations support the conclusion that the integrated IR spectra of fluorinated ethers are more intense than those of analogous alkanes.

Figs. (**3**, **4** and **5**) present experimental spectra for fluorinated alkanes and analogous ethers. Computed IR spectra are superimposed on the experimental spectra for comparison. In general, the computations predict peaks at or near the wavenumber at which experimental peaks appear, and qualitatively reproduce the relative heights, or intensities, of the peaks. It has been generally observed that vibrational frequencies obtained by computational approaches require scaling to match experiment [21]; this scaling is typically accomplished by multiplication of

frequencies by a factor which differs according to method and basis set but is generally slightly less than 1. In this case, however, scaling would clearly have a detrimental effect on the agreement of theory and experiment.

Fig. (**3**) shows spectra of CF_3CH_3 and CF_3OCH_3. In the case of CF_3CH_3, the wavenumbers of experimental IR peaks are well matched by computed peaks, and the relative intensities of the calculated modes are in general agreement with experiment. The experimental and computed spectra of CF_3OCH_3 are also in good agreement. Most experimental absorbances may be assigned to one computed mode, but an experimental peak at 1190 cm^{-1} may be thought to arise from two modes, modes our computations assign wavenumber frequencies of 1144 and 1177 cm^{-1}.

Fig. (**4**) displays experimental and calculated spectra of CF_3CF_2H and CF_3OCF_2H. The spectrum of CF_3CF_2H displays very good agreement between the wavenumbers of observed peaks and computed vibrational modes. Most experimental peaks correspond to one computed mode. Calculation suggests that one experimental peak at 1210 cm^{-1} may arise from two modes – the B3LYP/6-311G(2d,2p) calculation determines these modes to be at 1188 and 1206 cm^{-1}. The relative intensities of observed absorbances are also reproduced by the calculations.

Table 1. Calculated Vibrational Mode Data for CF_3OCH_3. Frequency (cm^{-1}), Intensity (KM/mol) and Irreducible Representation ("Irrep") of Each Mode are Displayed

Point group	C_s		
Mode	**Frequency (cm^{-1})**	**Intensity (KM/mole)**	**Irrep**
1	102.8455	2.3416	A"
2	169.2162	2.6189	A"
3	270.8083	4.5735	A'
4	428.1435	0.2067	A"
5	443.3161	5.3928	A'
6	580.8619	7.6788	A'
7	608.4573	1.4520	A"
8	656.0349	0.4211	A'
9	838.2863	8.3070	A'
10	1069.3876	33.1635	A'
11	1144.8144	341.6713	A"
12	1177.7678	159.5930	A'
13	1180.1872	4.1002	A"
14	1249.8973	190.9129	A'
15	1291.1719	521.2602	A'
16	1492.6496	28.5025	A'
17	1499.7863	4.1599	A"
18	1511.0472	19.9171	A'
19	3057.6750	24.8581	A'
20	3129.0874	16.3197	A"
21	3167.1768	9.4001	A'

Table 2. Calculated Vibrational Mode Data for CF_3CH_3. Frequency (cm^{-1}), Intensity (KM/mol) and Irreducible Representation ("Irrep") of Each Mode are Displayed

Point group	C_{3v}		
Mode	**Frequency (cm^{-1})**	**Intensity (KM/mole)**	**Irrep**
1	215.3777	0.0000	A_2
2	360.4157	0.5636	E
3	360.4180	0.5632	E
4	532.1031	0.6164	E
5	532.1048	0.6172	E
6	592.9739	20.0174	A_1
7	825.9967	4.5571	A_1
8	967.8262	63.2752	E
9	967.8436	63.2423	E
10	1229.7347	214.6035	E
11	1229.7972	214.6176	E
12	1281.9552	163.7336	A_1
13	1428.9812	77.6058	A_1
14	1486.9411	0.5006	E
15	1486.9421	0.5009	E
16	3074.6659	0.6521	A_1
17	3153.7227	5.3224	E
18	3153.7259	5.3201	E

Table 3. Calculated Vibrational Mode Data for CF_3OCF_2H Conformers. Frequency (cm^{-1}), Intensity (KM/mol) and Irreducible Representation ("Irrep") of Each Mode are Displayed

	Conformer 1			Conformer 2		
Point group	**C₁**			**C₁**		
Mode	**Frequency (cm^{-1})**	**Intensity (KM/mol)**	**Irrep**	**Frequency (cm^{-1})**	**Intensity (KM/mol)**	**Irrep**
1	34.6328	0.5847	*C₁*	29.0592	1.2676	*C₁*
2	116.9270	0.9667		72.4722	0.1758	
3	185.1446	0.2109		192.5289	2.3800	
4	348.1465	0.2830		352.4635	0.1220	
5	357.2944	0.2016		372.0863	0.5131	
6	502.5844	0.1456		455.6153	3.9255	
7	516.1444	3.9617		514.0684	2.9585	
8	580.2568	3.7716		585.4060	8.9714	
9	598.7415	17.5815		613.0644	3.7122	
10	634.7807	8.9575		655.2620	6.2636	
11	808.6871	27.5459		717.9024	12.8965	
12	840.6765	13.4829		907.2831	78.0883	
13	1081.5008	189.7208		1091.2452	285.9720	
14	1113.3428	137.1986		1121.3989	104.3745	
15	1144.0875	250.8496		1159.1950	236.2846	
16	1206.5129	433.4465		1182.7357	442.1670	
17	1218.8824	415.1468		1231.5262	373.4783	
18	1271.9252	408.6371		1300.4974	384.2171	
19	1381.1138	32.4193		1390.0975	45.4571	
20	1426.1840	41.6729		1428.7996	8.2197	
21	3151.4961	21.3588		3130.1854	17.8326	

Table 4.   Calculated Vibrational Mode Data for CF_3CF_2H. Frequency (cm^{-1}), Intensity (KM/mol) and Irreducible Representation ("Irrep") of Each Mode are Displayed

Point group	**C$_S$**		
Mode	**Frequency (cm^{-1})**	**Intensity (KM/mole)**	**Irrep**
1	64.6182	0.7848	A"
2	205.8253	2.2851	A"
3	239.2363	3.6431	A'
4	357.4182	0.0477	A'
5	410.3050	0.8440	A"
6	513.0201	6.9090	A'
7	570.7500	13.2191	A'
8	575.2809	0.4977	A"
9	716.6621	31.8403	A'
10	862.9864	45.9991	A'
11	1134.3085	98.6785	A"
12	1136.8769	130.4402	A'
13	1187.6755	195.6044	A'
14	1204.9731	360.2865	A"
15	1306.2303	145.4710	A'
16	1373.4765	7.1873	A"
17	1438.7735	0.7726	A'
18	3100.2398	19.7938	A'

Table 5.   Calculated Vibrational Mode Data for CF$_3$OCF$_2$CF$_2$H Conformers. Frequency (cm^{-1}), Intensity (KM/mol) and Irreducible Representation ("Irrep") of Each Mode are Displayed

	Conformer 1			Conformer 2		
Point group	**C$_1$**			**C$_1$**		
Mode	**Frequency (cm^{-1})**	**Intensity (KM/mole)**	**Irrep**	**Frequency (cm^{-1})**	**Intensity (KM/mole)**	**Irrep**
1	35.0326	0.1627	*C$_1$*	35.5712	0.0272	*C$_1$*
2	59.0553	0.7184		66.4939	1.1493	
3	88.1468	0.0834		91.0391	0.2070	
4	133.4210	0.7372		135.2615	0.6394	
5	211.0256	1.2143		206.3622	1.0889	
6	247.1508	2.0882		214.4308	2.1579	
7	312.9975	1.4489		334.9857	0.1717	
8	341.3613	0.8573		345.8128	0.3043	
9	354.4157	1.0326		364.1107	0.2116	
10	425.4664	1.3823		452.7500	0.1105	
11	505.8179	4.2338		520.6574	5.5810	
12	531.4008	0.9212		546.9576	6.8792	
13	557.0270	14.1182		560.1589	7.9298	
14	608.6853	5.5255		586.2555	55.9488	
15	638.9984	2.6682		630.2814	3.4643	
16	677.2749	13.7477		647.4391	7.9746	
17	790.5566	59.0787		760.7335	38.6658	
18	851.2707	22.6810		829.2702	2.4953	
19	907.0643	40.5334		964.4617	2.1461	
20	1111.6405	249.1341		1110.9638	329.8109	
21	1138.0969	80.5685		1133.4036	30.0983	
22	1148.0569	453.8026		1138.4121	132.2048	
23	1155.9705	167.5193		1160.3459	192.6040	
24	1216.6582	132.7238		1221.3180	519.8325	
25	1229.2760	488.4415		1229.9909	423.9226	
26	1254.6516	285.6867		1268.5272	508.1193	
27	1328.2648	308.9304		1310.0708	53.2860	
28	1375.2470	10.5269		1373.4133	9.5562	
29	1431.5737	3.3987		1436.2635	7.2735	
30	3102.3219	16.9444		3097.2670	18.5014	

Table 6.   **Calculated Vibrational Mode Data for $CF_3CF_2CF_2H$ Conformers. Frequency (cm^{-1}), Intensity (KM/mol) and Irreducible Representation ("Irrep") of Each Mode are Displayed**

	Conformer 1			Conformer 2		
Point group	C_s			C_1		
Mode	Frequency (cm^{-1})	Intensity (KM/mol)	Irrep	Frequency (cm^{-1})	Intensity (KM/mol)	Irrep
1	18.7521	0.3215	A"	43.8475	0.8176	*C_1*
2	94.3642	1.2037	A"	77.9294	0.4598	
3	159.5023	0.3154	A'	151.9656	1.0026	
4	211.3936	2.4294	A"	215.9412	3.5457	
5	217.2527	0.1772	A"	237.8643	2.1502	
6	276.0926	4.1858	A'	270.5530	1.1637	
7	331.6876	0.0131	A'	316.9001	0.4931	
8	365.1800	0.3698	A"	344.9278	0.0551	
9	369.0100	0.3138	A'	382.2249	0.7719	
10	498.1578	0.7277	A"	448.0799	3.2599	
11	516.3121	15.3319	A'	518.5032	10.8155	
12	555.5813	10.4475	A'	568.2713	2.9386	
13	596.0115	0.5057	A"	584.9568	4.3081	
14	607.6390	45.4794	A'	635.0028	7.2967	
15	701.5329	31.8089	A'	738.0897	37.2824	
16	773.5069	2.8535	A'	831.6396	52.0026	
17	1109.7708	68.6179	A'	1031.9058	194.0983	
18	1130.9818	46.4719	A"	1126.1856	59.6210	
19	1138.5059	147.9003	A'	1138.0923	71.7179	
20	1174.2100	150.0782	A"	1168.6061	136.7032	
21	1199.6784	244.5615	A'	1203.8594	294.2338	
22	1225.0681	385.0124	A"	1225.5769	264.8343	
23	1236.2790	70.4915	A'	1266.8306	113.9035	
24	1333.3357	85.5642	A'	1346.3336	46.8223	
25	1369.1067	16.5306	A"	1385.3947	19.0368	
26	1434.8419	3.4370	A'	1419.7105	18.2302	
27	3087.5365	18.4544	A'	3107.6426	14.4095	

The spectrum of CF_3OCF_2H displays the experimental IR cross sections and calculated spectra for both conformers. Weighting is assigned to the computed absorbances of the conformers by multiplying each by its relative fraction as determined by calculation of the Boltzmann ratio of the conformers at 298 K; i.e., we first compute the ratio of molecules in conformer 1 to conformer 2, N_1/N_2, by

$$N_1/N_2 = \exp[-(E_1 - E_2)/kT]$$

where $E_1 - E_2$ is the energy difference between conformer 1 and 2, k is the Boltzmann constant, and T is 298 K, a

temperature value equal or close to the temperature at which experiments were performed [18]. This ratio is then converted into relative fractions. This calculation assigns a fraction of 0.1516 to conformer 1 and 0.8484 to conformer 2.

Computations predict the small experimental peak at 907 cm^{-1} as arising from a mode in conformer 2, and experiment and calculation both place a group of peaks between 1080 cm^{-1} and 1450 cm^{-1}, with contributions from modes from both conformers. The observed peak at 1300 cm^{-1} seems to correspond to a mode in conformer 2, and a small observed
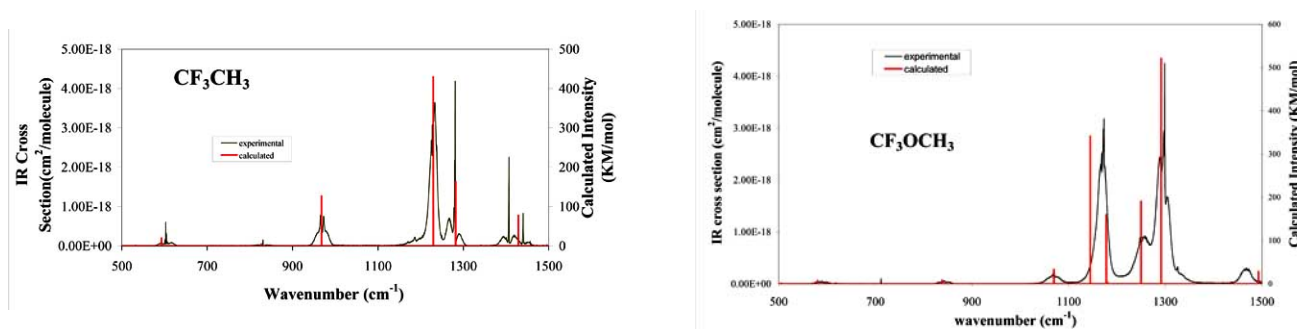
Fig. (3). Experimental and calculated IR spectra of CF_3CH_3 (left) and CF_3OCH_3 (right).
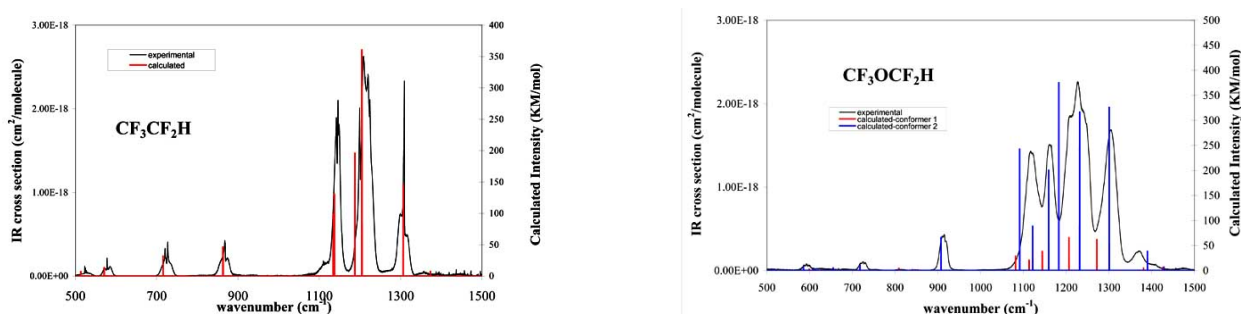

Fig. (4). Experimental and computed IR spectra of CF_3CF_2H (left) and CF_3OCF_2H (right).
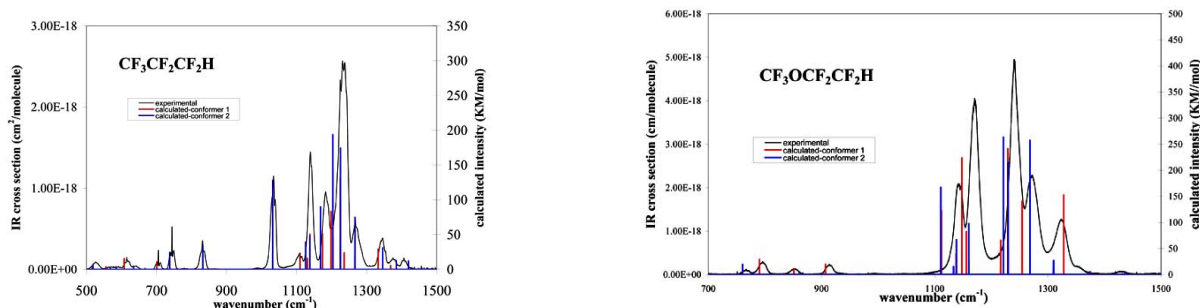
Fig. (5). Experimental and computed IR spectra of $CF_3CF_2CF_2H$ (left) and $CF_3OCF_2CF_2H$ (right).

peak at 1380 cm^{-1} may have contributions from modes in conformer 2 and conformer 1 The large observed peak at 1230 cm^{-1} may arise from contributions from intense modes in conformer 2 which computations place at 1182 cm^{-1} and 1231 cm^{-1} Other experimental peaks at 1124 cm^{-1} and 1166 cm^{-1} may be assigned to modes from conformer 2 as illustrated in the figure.

Fig. (**5**) displays the spectra of $CF_3CF_2CF_2H$ and $CF_3OCF_2CF_2H$. $CF_3CF_2CF_2H$ is predicted to exist as two conformers with conformer 2 the greater in energy by only 0.020 kcal/mol, but while conformer 1 has a mirror plane of symmetry, conformer 2 is chiral, one isomer of an enantiomer pair. Boltzmann ratio calculations of the ratio N_2/N_1 similar to the one discussed above for CF_3OCF_2H must thus include a factor of two, i.e.,

$$N_2/N_1 = 2\exp[-(E_2 - E_1)/kT]$$

This calculation assigns a fraction of 0.6591 to conformer 2 and 0.3409 to conformer 1. The spectrum of $CF_3CF_2CF_2H$ incorporates weighting for the relative amounts of the conformers and shows clear correspondence between observed peaks and computed modes in many instances, and observed peaks that cannot be attributed to one unique

computed mode may be explained as arising from contributions from 2 or more modes.

The molecule $CF_3OCF_2CF_2H$ is predicted in this work to exist as two conformers, with conformer 1 the greater in energy by only 0.016 kcal/mol. As both conformers are chiral, the computation of fractions follows as it did for CF_3OCF_2H, the ratio N_1/N_2 is

$$N_1/N_2 = \exp[-(E_1 - E_2)/kT]$$

and the resulting fractions are 0.4932 for conformer 1 and 0.5068 for conformer 2. Fig. (**5**) shows the IR spectrum with calculated peaks weighted for the contributions of the conformers. Small experimental absorbances in the range 700-900 cm^{-1} may be assigned to modes in either conformer 1 or conformer 2. The observed peak at 1329 cm^{-1} appears to arise from a mode in conformer 1, the experimental absorbance at 1275 cm^{-1} may be attributed to a mode in conformer 2, and the largest peak at 1241 cm^{-1} may be interpreted as arising from absorptions by modes in both conformers.

The relative IR intensities of vibrational modes are frequently discussed in terms of the change in the dipole moment of the molecule induced by the vibrational motion
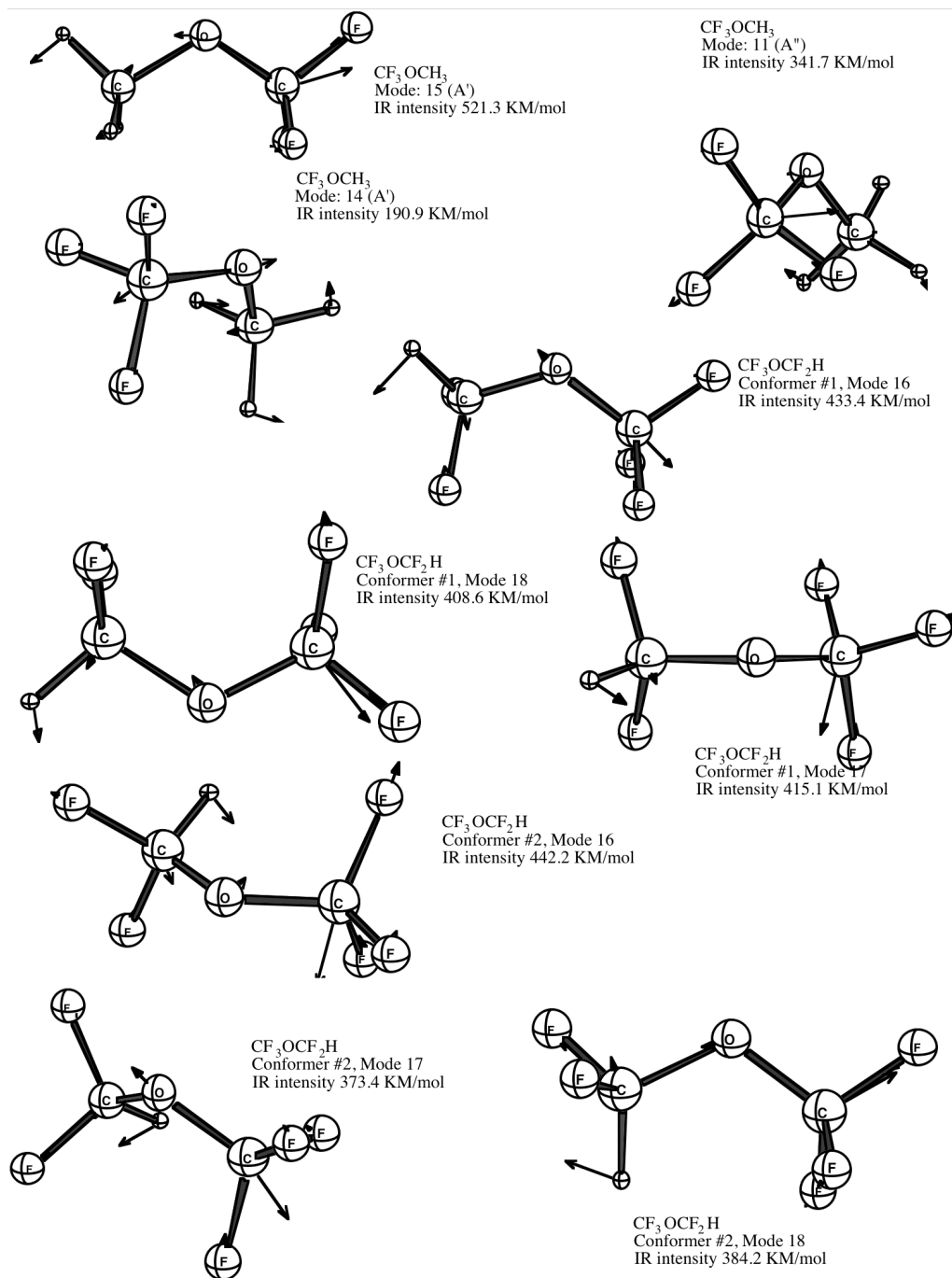
Fig. (6). Arrow projections of the three brightest vibrational modes of CF$_3$OCH$_3$ and both conformers of CF$_3$OCF$_2$H.

[22]. The larger the change in the dipole caused by a vibrational motion, the more intense the IR peak corresponding to that mode is expected to be. In the case of the ethers studied in this work, the most intense vibrational modes are uniformly associated with motions which serve to distort carbon-oxygen bonds within the ether, making the bonds alternately longer and shorter as the mode oscillates. Fig. (**6**) displays vector projections for the three brightest modes of CF$_3$OCH$_3$ and the conformers of CF$_3$OCF$_2$H; Fig. (**7**) displays the three brightest modes for CF$_3$OCF$_2$CF$_2$H. The two figures illustrate the C-O bond distortions associated with the brightest modes of the ethers.

CONCLUSION

Computations have determined the gas-phase IR spectra of several fluorinated ethers and their analogous alkanes, and these spectra have been compared to experimental measurements. The theoretical spectra reproduce the essential features of each of the measured absorption spectra. The good agreement between experiment and theory, both in terms of wavenumber location and relative intensities of peaks, suggests that the B3LYP/6-311G(2d,2p) calculations correctly describe the motions of each molecule associated with each vibrational mode. Examination of the vibrational modes and the corresponding nuclear motions clearly
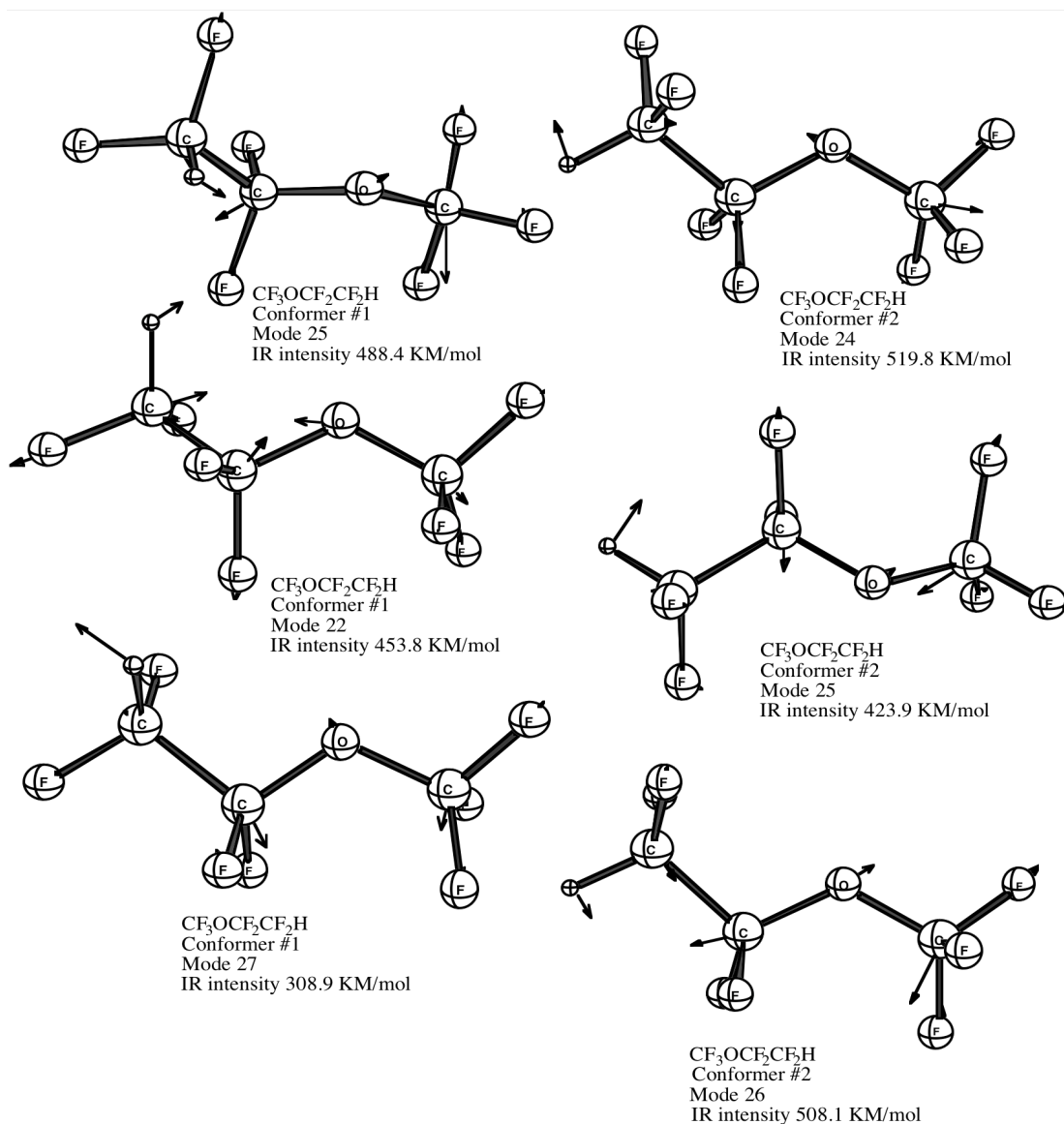
CF₃OCF₂CF₂H
Conformer #1
Mode 25
IR intensity 488.4 KM/mol

CF₃OCF₂CF₂H
Conformer #2
Mode 24
IR intensity 519.8 KM/mol

CF₃OCF₂CF₂H
Conformer #1
Mode 22
IR intensity 453.8 KM/mol

CF₃OCF₂CF₂H
Conformer #2
Mode 25
IR intensity 423.9 KM/mol

CF₃OCF₂CF₂H
Conformer #1
Mode 27
IR intensity 308.9 KM/mol

CF₃OCF₂CF₂H
Conformer #2
Mode 26
IR intensity 508.1 KM/mol

Fig. (7). Arrow projections of the three brightest vibrational modes of both conformers of $CF_3OCF_2CF_2H$.

indicates that the IR spectrum of each fluorinated ether studied has very intense peaks arising from modes involving distortion of carbon-oxygen bonds. The spectrum of each ether has more peaks, and brighter peaks, than that of its analogous alkane. This result may be true for a comparison of any fluorinated ether and its alkane.

While this study clearly shows that any given atmospheric concentration of fluorinated ethers would contribute more to global warming than the corresponding alkane. This study does not address other relevant issues such as the reactivity, fate, and relative atmospheric lifetimes of fluorinated ethers and alkanes, which must be considered for evaluation of the global warming impact of these compounds.

ACKNOWLEDGEMENTS

REFERENCES

[1]   Molina, M.J.; Rowland, F.S. Stratospheric sink for chlorofluoromethanes-chlorine atom catalyzed destruction of ozone. *Nature* (London), **1974**, *249*, 810.
[2]   Newman, P.A.; Oman, L. D.; Douglas, A. R.; Fleming, E. L.; Frith, S. M.; Hurwitz, M. M.; Kawa1, S. R.; Jackman, C. H.; Krotkov, N. A.; Nash, E. R.; Nielsen, J. E.; Pawson, S.; Stolarski, R. S.; Velders, G. J. M. What would have happened to the ozone layer if chlorofluorocarbons (CFCs) had not been regulated? *Atmos. Chem. Phys.*, **2009**, *9*, 2113-2128.
[3]   Wallington, T. J.; Schneider, W.F.; Sehested, J.; Nielsen, O.J. Hydrofluorocarbons and stratospheric ozone. *Faraday Discuss.*, **1995**, *100*, 55-64.
[4]   Young, C. J.; Hurley, M. D.; Wallington, T. J.; Mabury, S. A. Atmospheric Lifetime and Global Warming Potential of a Perfluoropolyether. *Environ. Sci. Technol.*, **2006**, *40*, 2242-2246.

[5]   Young, C.J.; Hurley, M.D.; Wallington, T. J. Molecular structure and radiative forcing of fluorinated ethers: a structure-activity relationship. *J. Geophys. Res*., **2008**, *113*, D24301.

[6]   Blowers, P.; Moline, D. M.; Tetrault, K. F.; Wheeler, R. R.; Tuchawena, S. L. Global warming potentials of hydrofluoroethers. *Environ. Sci. Technol.*, **2008**, *42*, 1301-1307.

[7]   Blowers, P.; Tetrault, K.F.; Trujillo-Morehead, Y. Global warming potential predictions for hydrofluoroethers with two carbon atoms. *Theor. Chem. Accounts,* **2008**, *119*, 369-381.

[8]   Blowers, P.; Moline, D.M.; Tetrault, K.F.; Wheeler, R.R.; Tuchawena, S.L. Prediction of radiative forcing values for hydrofluoroethers using density functional theory methods. *J. Geophys. Res.*, **2007**, *112*, D15108.

[9]   Good, D. A.; Francisco, J. S. Sstructure and vibrational spectra of chloroflurocarbon substitutes: an experimental and ab initio study of Fluorinated Ethers CHF_2OCF_3 (E125), CHF_2OCHF_2 (E134), and CH_3OCF_3 (E143A). *J. Phys. Chem. A*., **1998**, *102*, 1854-1864

[10] Good, D. A.; Francisco, J.S.; Jain A. K.; Wuebbles D. J. Lifetimes and global warming potentials for dimethyl ether and for fluorinated ethers: CH_3OCF_3 (E143a) CHF_2OCHF_2 (E134), CHF_2OCF_3 (E125). *J. Geophys. Res. Atmos*., **1998** *103*(D21), 28181-28186.

[11] Zhang, Z.; Saini, R. D.; Kurylo, M. J.; Huie, R. E. Rate constants for the reactions of the hydroxyl radical with several partially fluorinated ethers. *J. Phys. Chem.,* **1992**, *96*, 9301

[12] Hsu, K. J.; DeMore, W. B. Temperature-dependent rate constants and substituent effects for the reactions of hydroxyl radicals with three partially fluorinated ethers. *J. Phys. Chem*., **1995**, *99*, 11141.

[13] Cooper, D. L.; Cunningham, T. P.; Allan, N. L.; McCulloch, A. Tropospheric lifetimes of potential CFC replacements: Rate coefficients for reaction with the hydroxyl radical. *Atmos. Environ. Part A*., **1992**, *26*, 1331.

[14] Good, D. A.; Francisco, J. S. Bond dissociation energies and heats of formation for fluorinated ethers: E143A (CH_3OCF_3), E134 (CHF_2OCHF_2), and E125 (CF_3OCHF_2). *J. Phys. Chem. A.,* **1998**, *102*, 7143-7148.

[15] See Stevens, J. E.; Jabo Khayat, R. A.; Radkevich, O.; Brown, J. CF_3CFHO vs. CH_3CH_2O: An Ab initio molecular orbital study of mechanisms of decomposition and reaction with O_2. *J. Phys. Chem. A*., **2004**, *108*, 11354-11361, and references therein.

[16] Christidis, N.; Hurley, M.D.; Pinnock, S.; Shine, K.P.; Wallington, T. J. Radiative forcing of climate change by CFC-11 and possible CFC replacements. *J. Geophys. Res*., **1997**, *102*, 19597-19609.

[17] Sihra, K.; Hurley, M.D.; Shine, K. P.; Wallington, T. J. Updated radiative forcing estimates of sixty-five halocarbons and non-methane hydrocarbons. *J. Geophys. Res*., **2001**, *106*, 20493.

[18] Sulbaek Andersen, M. P.; Nielsen, O. J.; Wallington, T. J.; Hurley, M.D.; DeMore, W. B. Atmospheric Chemistry of $CF_3OCF_2CF_2H$ and $CF_3OC(CF_3)_2H$: Reaction with Cl Atoms and OH radicals, degradation mechanism, global warming potentials, and empirical relationship between k(OH) and k(Cl) for organic compounds. *J. Phys. Chem. A*., **2005**, *109*, 3926.

[19] Becke, A. D. Density-functional thermochemistry. I. The effect of the exchange-only gradient correction. *J. Chem. Phys*., **1992**, *96*, 2155-2160; Becke, A. D. Density-functional thermochemistry. III. The role of exact exchange. *J. Chem. Phys*., **1993**, *98*, 5648-5652.

[20] Frisch, M. J.; Trucks, G. W.; Schlegel, H. B.; Scuseria, G. E.; Robb, M. A.; Cheeseman, J. R; Montgomery, J. A., Jr.; Vreven, T.; Kudin, K. N.; Burant, J. C.; Millam, J. M.; Iyengar, S. S.; Daniels, A. D.; Tomasi, J.; Barone V.; Menucci, B.; Cossi, M.; Scalmani, G.; Rega, M; Petersson, G. A.; Nakatsuji, H.; Hada, M.; Ehara, M.; Toyota, K.; Fukuda, R.; Hasegawa, J.; Ishida, M.; Nakajima, T.; Honda, Y.; Kitao, O.; Nakai, H.; Klene, M.; Li, X.; Knox, J. E.; Hratchian, H. P.; Cross, J. B.; Adamo, C.; Jaramillo, J.; Gomperts, R.; Stratmann, R. E.; Yayev, O.; Austin, A. J.; Cmmi, R.; Pomelli, C.; Ochterski, J. W.; Ayala, P. Y.; Morokuma, K.; Voth, G. A.; Salvador, P.; Dannenberg, J. J.; Zakrewski, V. G.; Dapprich, S.; Daniels, A. D.; Strain, M. C.; Farkas, O.; Malick, D. K.; Rabuck, A. D.; Raghavachari, K.; Foresman, J. B.; Ortiz, J. V.; Cui, Q.; BAboul, A. G.; Clifford, S.; Cioslowski, J.; Stefanov, B. B.; Liu, G.; Liashenko, A.; Piskorz, P.; Komaromi, I.; Martin, R. L.; Fox, D. J.; Keith, T.; Al-Laham, M. A.; Peng, C. Y.; Nanayakkara, A.; Challacombe, M.; Gill, P. M. W.; Johnson, B.; Chen, W.; Wong, M. W.; Gonzales, C.; Pople, J. A. Gaussian 03, Revision C.02. Gaussian, Inc., Wallingford, CT, **2004**.

[21] Scott, A. P.; Radom, L. Harmonic vibrational frequenices: an evaluation of hartree-fock, moller-plesset, quadratic configuration interaction, density functional theory, and semiempirical scale factors. *J. Phys. Chem*., **1996**, *100*, 16502-16513.

[22] See, for example, Atkins, P. *Physical Chemistry*, 8th ed., W. H. Freeman and Company, New York, **2006**, p. 454.